Collisional ion-pair formation in an excited alkali-metal vapor

L. Barbier, M. T. Djerad, and M. Chéret
Service de Physique des Atomes et des Surfaces, Centre d'Etudes Nucléaires de Saclay, 91191 Gif-sur-Yvette Cedex, France
(Received 25 March 1985; revised manuscript received 20 March 1986)

Analysis of the negative-ion current in an excited rubidium vapor gives evidence for the following collisional reaction: $Rb(nl)+Rb(5s)\rightarrow Rb^+ + Rb^-$. Ion-pair formation is studied for a wide range of levels lying below ($5d$, $7s$, $6d$, $8s$) or above ($7d$, $9s$, $8d$, $10s$) the Coulomb potential curve limit. The rate coefficient increases from $(1.1\pm0.6)\times10^{-14}$ cm^3s^{-1} for the $5d$ level to $(1.1\pm0.3)\times10^{-12}$ cm^3s^{-1} for the $6d$ level and then decreases to approximatively 6×10^{-14} cm^3s^{-1} for the $9s$ level. For the $5d$ and $7s$ levels a Landau-Zener-type formalism accounts well for the experimental results. A model is proposed for the other states.

I. INTRODUCTION

Ion-pair production by collision between ground-state and excited atoms according to

$$A^* + A \rightarrow A^+ + A^- \quad (1)$$

is regarded as a possible reaction to explain positive ion formation in an alkali-metal vapor.[1-3] No clear experimental evidence for this process has, however, been established up to now.

This reaction has been considered in the framework of a general study of collisional ionization of excited rubidium atoms.[4] Resonant $Rb(5p)$ atoms and highly excited $Rb(nl)$ atoms are formed in a cell by means of cw lasers. Analysis of positive-ion currents allowed the following processes to be characterized as the main reactions producing ions: Hornbeck-Molnar ionization, according to

$$Rb(nl)+Rb(5s)\rightarrow Rb_2^+ + e^- , \quad (2)$$

Penning ionization, between two excited atoms

$$Rb(nl)+Rb(5p)\rightarrow Rb^+ + e^- + Rb(5s) , \quad (3)$$

and photoionization by the excitation lasers,

$$Rb(nl)+h\nu\rightarrow Rb^+ + e^- . \quad (4)$$

It is concluded from these previous investigations that ion-pair formation can only be studied by a direct observation of negative ions. In a first study,[5] Rb^- ions have been detected after the excitation of the $6d\,^2D_{5/2}$ state. The corresponding current was at least 3 orders of magnitude lower than the Rb^+ current. A thorough analysis of the Rb^- current showed that it corresponds to the reaction

$$Rb(6d\,^2D_{5/2})+Rb(5s)\rightarrow Rb^+ + Rb^- . \quad (5)$$

The associated rate coefficient $K^-(6d)$ was determined equal to $(1.1\pm0.6)\times10^{-12}$ cm^3s^{-1}. Such a value cannot be explained by a transition at the crossing point between the ionic and covalent curves, the Landau-Zener probability being negligible.

In the present paper ion-pair formation is studied more extensively for various excited rubidium levels. Some of these levels lie below the asymptotic limit of the ionic curve [Rb electron affinity 3919.2 cm^{-1} (Ref. 6)] while others are lying above this limit. A theoretical model is proposed to explain the experimental results.

The paper is organized as follows. The experimental method is briefly described in Sec. II while Sec. III lists all the checks that have been made in order to discard various possible reactions.[7] Section IV discusses the determination of the rate coefficients as deduced from the data. Section V provides the details needed in order to obtain the rate coefficients for the individual levels. Section VI indicates under what assumption cross sections can be obtained. Finally, Sec. VII deals with theoretical calculations and puts the obtained results in a general perspective before some final remarks end the paper.

II. EXPERIMENTAL METHOD

The experimental setup (Fig. 1) has already been described in detail;[4] only the modifications needed to detect negative ions are presented in this paper.

Two multimode low-power cw dye laser beams cross at the center of a cylindrical cell ($T_{reservoir}=335$ K, $T_{cell}=453$ K, Rb concentration 10^{12} cm^{-3}). The first laser beam (ir,$\lambda=780$ nm) pumps the resonant state $Rb(5p\,^2P_{3/2})$ (concentrations 10^{10} cm^{-3}) and the second (λ varying from 741—539 nm) populates a highly excited state $Rb(nl)$ ($l=s$ or d from $5d$ to $10s$, concentration $\sim10^8$ cm^{-3}). For the lowest levels ($5d$ and $7s$) the two dye lasers are pumped with the same Kr^+ laser (pumping power ~7 W).

The ions are mass analyzed by means of a quadrupole spectrometer system. Positive and negative ions are alternately measured by inverting ion optics and electron multiplier polarities.[8] The detector is used in the analog mode. The negative-ion current is very low (10^{-14} A), but can be separated from the electron current (10^{-10} A), associated with positive ions, by mass analysis. The total positive-ion current is measured between two polarized plates using a picoammeter. The transmission factor of the mass analysis system must be determined for each ion species Rb^+,Rb_2^+,Rb^-. This is done using the same amplification factor on the electron multiplier and with the same voltages on the ion optics: Only the transmission of

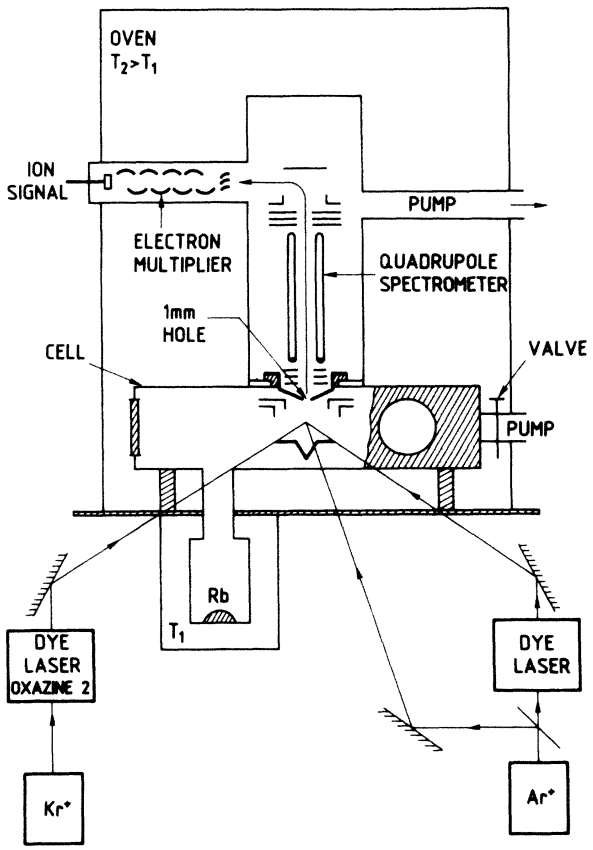

FIG. 1. Experimental setup.

the mass spectrometer and the ion-e^- conversion factor change with the ion species. The electron multiplier output current is measured for Rb^+ and Rb_2^+ ions by changing the experimental conditions in the cell in such a way that either the Hornbeck-Molnar process (i.e., Rb_2^+ ions) or Penning and photoionization processes (i.e., Rb^+ ions) are dominant. The transmission factor of the whole system is 1.6 times higher for Rb_2^+ ions. The transmission factor of the mass analyzer is the same for Rb^+ and Rb^- ions. The conversion efficiency of the first dynode is measured for Rb^+ and Rb^- ions by varying the applied voltage and keeping the gain constant. At high energy (Rb^+ 2400 eV, Rb^- 1800 eV) the output current becomes constant. This corresponds to the saturation of the conversion factor. Under these conditions the efficiency is the same for both ions.[9]

Under the usual experimental conditions the Rb^+ current is much higher than the Rb^- current. To ensure a good linearity of the system over 5 orders of magnitude Rb^+ ions are measured with a lower electron multiplier gain (attenuation of ~ 130). The electronic system (preamplifier and multichannel analyzer) is used under the same conditions for both ions. The Rb^+ signal is accumulated over 500 mass scanning and the Rb^- signal over 20 000 scanning.

III. EXPERIMENTAL CHECKS

It is worth recalling the various experimental checks[5] that have been performed for all the studied levels ($5d, 7s, 6d, 8s, 7d, 9s, 8d, 10s$). They allow us to conclude that the negative-ion formation is due to collisions between Rb(nl) and Rb($5s$) atoms. These tests include the variation of numerous experimental parameters (tuning and power of both lasers, cell temperature, and consequently Rb_2 density, Rb reservoir temperature and consequently Rb pressure) as well as the use of an additional electron source. More precisely we have verified the following:

(1) Both lasers need to be tuned to the atomic transitions to produce negative ions. This eliminates the reaction

$$Rb_2 + h\nu \rightarrow Rb^+ + Rb^- \tag{6}$$

and indicates that the Rb(nl) level must be populated, eliminating the reaction

$$Rb(5p) + Rb(5p) \rightarrow Rb^+ + Rb^- . \tag{7}$$

It should be noted that the internal energy of the two colliding partners and the product of their concentration are the same as in Rb($5d$)+Rb($5s$) collisions.[10]

(2) The intensity of the Rb^- signal varies linearly with the different laser power. This eliminates the exoergic reaction:

$$Rb(nl) + Rb(n'l') \rightarrow Rb^+ + Rb^- \tag{8}$$

($n'l'$ being the same excited state as nl or $5p$ or any excited state populated by radiative cascade), as well as other reactions involving two particles produced by Penning or Hornbeck-Molnar reactions such as

$$Rb_2^+ + e^- \rightarrow Rb^+ + Rb^- . \tag{9}$$

(3) The dissociative attachment of an electron on a Rb_2 molecule

$$Rb_2 + e^- \rightarrow Rb^+ + Rb^- \tag{10}$$

is eliminated by adding an external electron source.[5]

(4) Finally, production of a negative ion by collision between an excited atom Rb(nl) and a ground-state molecule

$$Rb(nl) + Rb_2 \rightarrow Rb^- + Rb_2^+$$
or
$$Rb^- + Rb^+ + Rb \tag{11}$$

is discarded by varying the cell temperature at a constant Rb reservoir temperature.

It is concluded from all the above presented checks that for all the levels investigated Rb^- formation is due to the collision between a highly excited atom and a ground-state atom according to

$$Rb(nl) + Rb(5s) \rightarrow Rb^+ + Rb^- . \tag{12}$$

Note finally that the study of the variation of the Rb^- current with the cell temperature is of great interest. Its decrease from 453–383 K corresponds to an increase in the Rb_2 concentration by a factor of 10. We observe that

as the Rb_2 concentration increases the Rb^- current remains approximately constant for the $7d$, $9s$, $8d$, and $10s$ levels and decreases for the $5d$, $7s$, $6d$, and $8s$ levels. In fact, the decay is so fast for the $5d$ level that the signal disappears as soon as the temperature is made to decrease from 450–420 K. These variations completely discard all reactions involving Rb_2 molecules. They are in agreement with the energy balance of Eq. (12) for all levels. The quantitative analysis of this effect is presented later (Fig. 4).

IV. DETERMINATION OF RATE COEFFICIENTS

The rate coefficient for ion-pair formation for a given $Rb(nl)$ level is deduced either from the $I(Rb^-)/I(Rb_2^+)$ ratio or from the $I(Rb^-)/I(Rb^+)$ ratio depending upon the level under consideration.

A. Case I ($6d$ to $10s$ levels)

Rb_2^+ ions are formed by the Hornbeck-Molnar process

$$Rb(nl)+Rb(5s)\rightarrow Rb_2^+ + e^- \ . \tag{2}$$

Ion-pair formation and the Hornbeck-Molnar process involve the same colliding partners. The corresponding rate coefficients $K^-(nl)$ and $K_{HM}(nl)$ are related by

$$K^-(nl)=K_{HM}(nl)\frac{I(Rb^-)}{I(Rb_2^+)} \ , \tag{13}$$

where $I(Rb^-)$ and $I(Rb_2^+)$ are the ion currents at the electron multiplier output (taking into account the relative transmission for the two ion species).

B. Case II ($5d$ and $7s$ levels)

The above method fails in the case of the $5d$ and $7s$ levels because for these levels the Hornbeck-Molnar reaction is energetically forbidden. Thus the Rb^- current $I(Rb^-)$ is compared with the Rb^+ current, $I_{coll}(Rb^+)$ due to the Penning ionization

$$Rb(nl)+Rb(5p)\rightarrow Rb^+ + e^- + Rb(5s) \ . \tag{3}$$

The rate coefficient for ion-pair formation $K^-(nl)$ is then deduced from the known rate coefficients for Penning ionization[4] $K_{PI}(nl)$ using the following formula:

$$K^-(nl)=K_{PI}(nl)\frac{I(Rb^-)}{I_{coll}(Rb^+)}\frac{[5p]}{[5s]}\frac{V'}{V} \ , \tag{14}$$

where $[5p]$ and $[5s]$ are, respectively, the concentration of the resonant and ground-state atoms, and V' and V are the respective volumes in which the two reactions occur.

A thorough study of the reaction producing positive ions has already been performed.[4] Analysis of the Rb^+ current has shown that under our experimental conditions the main processes involved are Penning ionization and photoionization by the laser beams. Experimental techniques have allowed us to separate the contribution of the different processes and thus to know $I_{coll}(Rb^+)$ for the various experimental conditions (i.e., laser powers and Rb pressure). The $[5p]$ concentration is accurately determined from photoionization current of the resonant atoms near the threshold. For this purpose the 465-nm line of the Ar^+ laser is used. A careful analysis of the interaction volumes is made taking radiation trapping effects into consideration. The spatial distribution of the power in the laser beams is assumed to be Gaussian and in spite of the trapping the $[5p]$ distribution is also experimentally determined to be Gaussian.[10] These calculations and measurements allow V'/V (Refs. 4 and 10) to be accurately determined. Uncertainties in the $K^-(5d)$ and $K^-(7s)$ values obtained using the procedure described here are similar to those encountered when employing the previous method [Eq. (13)].

As for positive ions, the rate coefficients obtained from these measurements are effective coefficients.[4] The different levels below the laser excited level are populated by radiative cascade and thus can also participate in ion-pair formation. In Table I we report the densities $\rho(n'l',nl)$ of

TABLE I. Densities of the radiatively populated levels $n'l'$ for the various excited levels nl. The figures are deduced from the radiative model already used in Ref. 4.

nl / $n'l'$	$10s$	$8d$	$9s$	$7d$	$8s$	$6d$	$7s$	$5d$
$10s$	1							
$8d$	0	1						
$9p$	0.192	0.042						
$6f$	0	0.020						
$9s$	0.007	0.001	1					
$7d$	0.016	0.004	0	1				
$8p$	0.098	0.005	0.305	0.060				
$5f$	0.000	0.010	0	0.021				
$8s$	0.007	0.001	0.016	0.003	1			
$6d$	0.023	0.005	0.039	0.008	0	1		
$7p$	0.092	0.026	0.197	0.015	0.484	0.123		
$4f$	0.001	0.004	0.001	0.008	0	0.019		
$7s$	0.011	0.009	0.022	0.002	0.042	0.011	1	
$5d$	0.042	0.018	0.078	0.011	0.113	0.029	0	1
$6p$	0.111	0.067	0.214	0.069	0.381	0.059	0.833	0.278
$6s$	0.023	0.012	0.045	0.013	0.078	0.013	0.143	0.048
$4d$	0.028	0.032	0.052	0.038	0.083	0.043	0.125	0.052

the radiatively populated levels for each of the given excited Rb(nl) levels. These densities are calculated using the Einstein coefficients $A_{i\to j}$ (Refs. 11–13) such that

$$\rho(n'l',nl)=\frac{\sum_p A_{p\to n'l'}\rho(p,nl)}{\sum_q A_{n'l'\to q}}\ , \tag{15}$$

where p and q, respectively, indicate levels above and below the considered Rb($n'l'$) level.

The effective rate coefficients, $K^-(nl)$, can be expressed as follows in terms of the individual rate coefficients $k^-(nl)$:

$$K^-(nl)=\sum_{n'l'}^{nl} k^-(n'l')\rho(n'l',nl)\ . \tag{16}$$

Finally, $k^-(nl)$ values are deduced from $K^-(nl)$ by inverting this relation (see below).

V. DATA ANALYSIS

Negative ions are detected after excitation of the $5d$, $7s$, $6d$, and $8s$ levels that lie below the limit of the ionic curve. The reaction corresponds to a threshold energy defect varying between 4070 and 725 cm^{-1} (13–2.3 kT at 453 K). Negative ions are also observed when one of the $7d$, $9s$, $8d$, or $10s$ levels is excited. These levels lie above the Rb^+-Rb^- limit. The levels studied are represented on Fig. 2 together with the asymptotic Coulombic Rb^+-Rb^- curve.

Effective rate coefficients deduced from the measurements are given in Table II. It is worth noting that they vary over 2 orders of magnitude. The individual rate coefficients reported are deduced from the $K^-(nl)$ values by the following method.

As no information on p and f levels is available, it is first assumed that the individual rate coefficients are only dependent on the energy of the level and consequently weakly dependent on the orbital quantum number. As high l value levels ($l>3$) are weakly populated (Table I) we assume the system to be mainly governed by s, p, and d levels.

Ion-pair formation associated with excited atoms in a level below the $5d$ level presents a very high endothermicity. The contribution of these levels to the negative-ion current is consequently negligible. Thus we may write $k^-(5d)=K^-(5d)$ and $k^-(7s)=K^-(7s)$. When the $6d$ level is excited the contribution of $5d$ and $7s$ levels to the negative current proportional to $k^-(5d)\rho(5d,6d)+k^-(7s)\rho(7s,6d)$ is negligible. According to $\rho(n'l',6d)$ values Rb^- ions are mainly formed by the $6p$ and $7p$ levels and consequently:

$$K^-(6d)=k^-(6d)+\rho(7p,6d)k^-(7p)\ .$$

If we assume that $k^-(7p)=k^-(6d)$ a common value of 1.0×10^{12} $cm^3\ s^{-1}$ is obtained. This value used to solve the system associated with the highest states ($9s$, $8d$, and $10s$) gives a contribution of the $6d$ and $7p$ levels predominant and yields a calculated current higher than the measured value. The $k^-(7p)$ value is then certainly overestimated. A new value is chosen for the rate coefficient so that the currents corresponding to the excitation of the $8d$ and $10s$ levels are explained by the cascading process. We may then determine $k^-(nl)$ values for each level. The values obtained are given in Table II and in Fig. 3. In the table the total contribution of the radiatively populated levels $\alpha(nl)$ defined by

$$\alpha(nl)=\sum_{n'l'<nl} k^-(n'l')\rho(n'l',nl) \tag{17}$$

is also indicated.

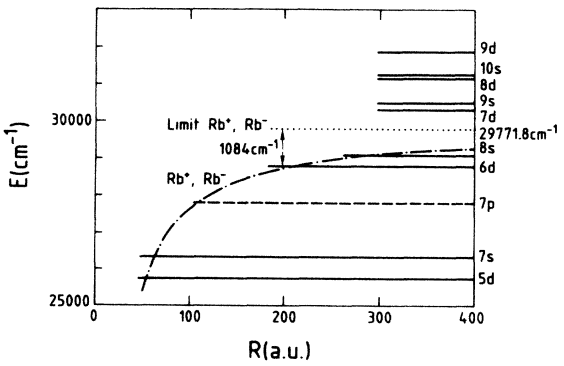

FIG. 2. Relative position of the levels studied and of the Coulombic Rb^+,Rb^- curve.

TABLE II. Effective, $K^-(nl)$ and individual, $k^-(nl)$ ion-pair formation rate coefficients. $\alpha(nl)$ is the contribution to the effective rate coefficient of the levels populated by radiative cascade.

Level	$K^-(nl)$ (cm^3s^{-1})	$k^-(nl)$ (cm^3s^{-1})	$\alpha(nl)$ (cm^3s^{-1})
$5d$	$(1.1\pm0.6)\times10^{-14}$	$(1.1\pm0.6)\times10^{-14}$	0
$7s$	$(1.0\pm0.5)\times10^{-13}$	$(1.0\pm0.5)\times10^{-13}$	0
$7p$		3×10^{-13}	
$6d$	$(1.1\pm0.3)\times10^{-12}$	$(1.1\pm0.3)\times10^{-12}$	4.2×10^{-14}
$8s$	$(5.4\pm1)\times10^{-13}$	3.9×10^{-13}	1.5×10^{-13}
$7d$	$(1.1\pm0.3)\times10^{-13}$	$(8\pm3)\times10^{-14}$	2.4×10^{-14}
$9s$	$(2.\pm0.7)\times10^{-13}$	$<6\times10^{-14}$	1.4×10^{-13}
$8d$	$(2.\pm0.8)\times10^{-14}$	$<10^{-14}$	2×10^{-14}
$10s$	$(8.\pm2)\times10^{-14}$	$<10^{-14}$	8×10^{-14}

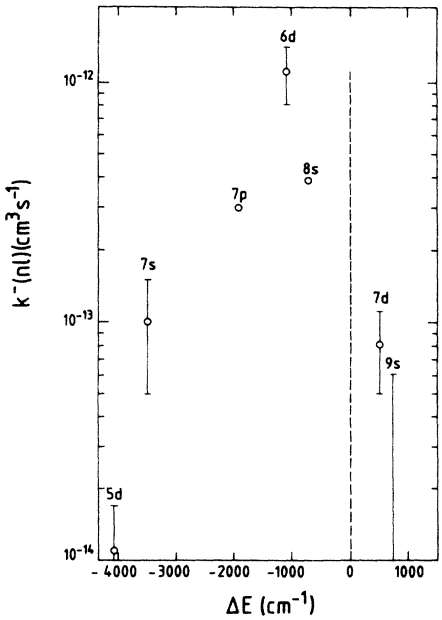

FIG. 3. Individual rate coefficients of the levels studied.

This coefficient is not too large for the $5d$, $7s$, and $6d$ levels below the ionic limit and for the $7d$ level above this limit. We therefore conclude that the $k^-(nl)$ values are correctly determined. The $k^-(nl)$ values for the $7p$, $8s$, and $9s$ levels are more dependent on our hypothesis.

VI. CROSS SECTIONS

The measurements are made in a cell containing atoms with a Maxwellian velocity distribution $M(v)$ represented by

$$M(v)=\left[\frac{\mu}{2\pi kT}\right]^{3/2} e^{-\mu v^2/2kT}4\pi v^2 .$$

The rate coefficient $k^-(nl)$ is often related to an averaged cross section $Q^-(nl)$ as follows:

$$k^-(nl)=Q^-(nl)\int_0^\infty M(v)v\,dv .$$

However, for the levels below the ionic limit ($5d$, $7s$, $6d$, and $8s$) the reaction is endothermic and only those atoms with a velocity large enough to balance the energy defect of the process can participate in the reaction. The proportion of atoms fulfilling this condition is

$$r=\int_{v_0}^\infty M(v)dv ,$$

where v_0 is the velocity of atoms at the threshold energy.

At 453 K, r is, respectively, equal to 0.20, 0.011, 6.25×10^{-3}, and 9.1×10^{-6} for the $8s$, $6d$, $7s$, and $5d$ levels; obviously $r=1$ for the $7d$ to $10s$ levels.

The rate coefficient expresses the efficiency of the reaction throughout the medium and is generally temperature dependent. The cross section represents the efficiency of the reaction in a binary collision and is velocity dependent. It is obviously zero below the ionic limit. Above the threshold the simplest assumption is that the cross section has a constant value $\sigma^-(nl)$. We then have

$$k^-(nl)=\sigma^-(nl)\int_{v_0}^\infty M(v)v\,dv . \tag{18}$$

For the levels above the ionic limit v_0 is equal to 0 and $\sigma^-(nl)$ is the averaged cross section $Q^-(nl)$ which is commonly considered to be the cross section at the mean velocity

$$\bar{v}=\int_0^\infty M(v)v\,dv .$$

For the levels below the ionic limit $\sigma^-(nl)$ can be considered to be the cross section near the threshold velocity v_0 as most of the efficient atoms are in a small velocity range above v_0. The values deduced from (18) are reported in Table III together with v_0 or $\bar{v}$.

Varying the cell temperature results in negligible changes in the mean velocity of the atoms but leads to a large change in the total number of reacting atoms especially at high-energy threshold. Individual rate coefficients are calculated at various temperatures using the $\sigma^-(nl)$ values deduced at 453 K. In Fig. 4 calculations and measurements for $7s$, $6d$, and $7d$ levels are presented. These levels correspond to typical examples encountered: high-energy threshold, medium-energy threshold, and exothermic reaction. Calculations and measurements agree well in every case. At 453 K, $k^-(5d)$ is already low. As the number of the reacting atoms decreases by a factor of 2.5 when the temperature is reduced to 420 K, it is therefore not surprising that the negative-ion signal disappears. These results show that $\sigma^-(nl)$ is a realistic value of the

TABLE III. Averaged cross sections $Q^-(nl)=[k^-(nl)]/\bar{v}$ ($\bar{v}$ mean velocity of the atoms) and ion-pair formation cross sections: $\sigma^-(nl)=[k^-(nl)]/\int_{v_0}^\infty M(v)v\,dv$ (v_0 velocity of the atoms at the threshold energy of the reaction). $Q^-(nl)=\sigma^-(nl)$ when the reaction is exoergic. $\bar{v}$ is then reported in the last column [Rb($7d$) and Rb($9s$)]. For the other levels the reaction is endoergic and v_0 is then reported.

Level	$Q^-_{nl}(cm^2)$	$\sigma^-_{nl}(cm^2)$	v_0 or $\bar{v}(cm\,s)$
$5d$	$(2.3\pm1.1)\times10^{-19}$	$(7.5\pm4)\times10^{-15}$	1.7×10^5
$7s$	$(2.1\pm1.1)\times10^{-18}$	$(1.1\pm0.5)\times10^{-14}$	1.6×10^6
$7p$	6.4×10^{-18}	4.1×10^{-16}	1.2×10^5
$6d$	$(2.3\pm0.6)\times10^{-17}$	$(1.7\pm0.5)\times10^{-16}$	8.7×10^4
$8s$	8.3×10^{-18}	2.5×10^{-17}	7.1×10^4
$7d$	$(1.7\pm0.6)\times10^{-18}$	$(1.7\pm0.6)\times10^{-18}$	4.7×10^4
$9s$	$<1.3\times10^{-18}$	$<1.3\times10^{-18}$	4.7×10^4

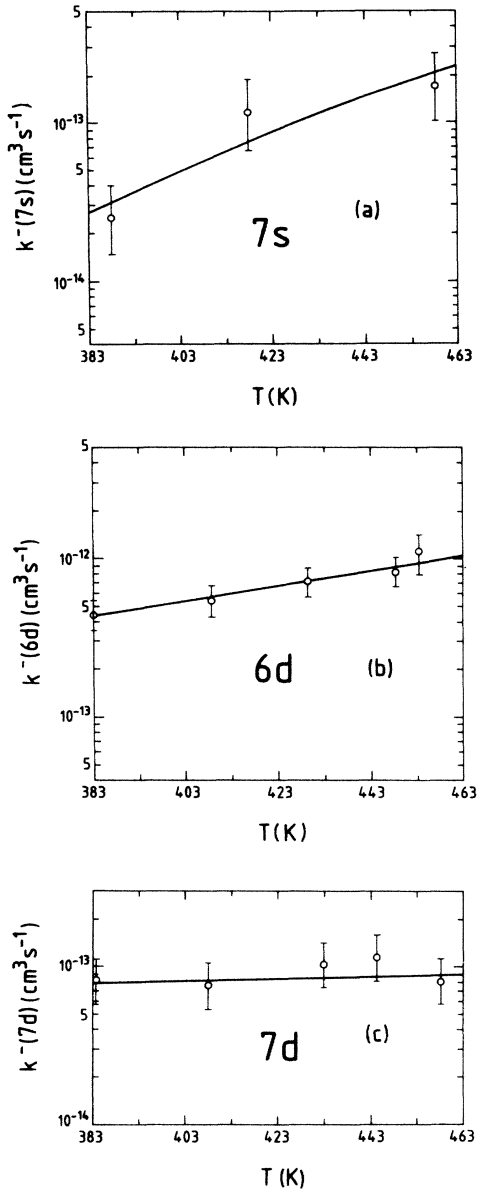

FIG. 4. Variation of the effective rate coefficient $K^-(nl)$ with cell temperature T_{cell} for the (a) $7s$, (b) $6d$, and (c) $7d$ levels, respectively.

cross section at thermal energies for the exothermic case and just above the threshold energy for the endothermic case.

VII. THEORETICAL ANALYSIS AND DISCUSSION

Most of the available experimental results on ion-pair formation are satisfactorily explained by the Landau-Zener-Stueckelberg (LZS) theory.[14] In this model the transition is localized at the crossing point R_c between the covalent and ionic curves and the transition probability P_{12} is equal to

$$P_{12}=e^{-2\pi H_{12}^2/v_c\Delta F}, \tag{19}$$

where v_c is the relative velocity of the atoms at R_c and ΔF is the difference between the slopes of the ionic and covalent curves at this point.

The total transition probability $P=2P_{12}(1-P_{12})$ is deduced from H_{12} and the parameters of the potential curves: R_c, ΔF, and v_c. The cross section can then be calculated by integrating P over the impact parameter b from 0 to the maximum value $b_{max}=R_c$. The rate coefficient is determined from formula (18).

In order to calculate the cross section we need to know the position of the crossing point, the shape of the i0nic and covalent curves at R_c, and the coupling H_{12}. In the Rb system the Coulombic curve $Rb^+ + Rb^-$ and the unperturbed covalent curve cross at large interatomic distances. It is therefore easy to determine R_c and ΔF using these potential curves (Table IV) (reported values of the velocity correspond to the threshold energy). H_{12} is therefore the only parameter that needs to be discussed.

Since the work of Landau-Zener and Stueckelberg, numerous atomic systems have been studied. They generally involve alkali-metal atoms (low-ionization potential) colliding with halogens[15] (high-electron affinity), oxygen,[16] or hydrogen.[17] A convenient representation of the dependence of the coupling on R_c is obtained by introducing the reduced parameters

$$H_{12}^*=\frac{2H_{12}}{\alpha\gamma}$$

and

TABLE IV. Experimental parameters for LSZ calculation. R_c is the crossing point between the covalent and the ionic curves. ΔF is the difference between the slopes of the covalent and the ionic curves. v_0 is the velocity of the atoms at the threshold energy of the reaction. H_{12} is the coupling between the covalent and the ionic curves. In the two last columns are $k_{LSZ}^-(nl)$ values calculated by LSZ method using H_{12} deduced from the Janev and Salin model (Ref. 21) and the individual rate coefficients $k^-(nl)$ deduced from the measurements.

Level	R_c (a.u.)	ΔF (a.u.)	v_0 (a.u.)	H_{12} (a.u.)	$k^-(nl)$ (cm^3s^{-1}) LZS calculations	$k^-(nl)$ (cm^3s^{-1}) Measurements
$5d$	53.93	3.44×10^{-4}	6.90×10^{-4}	9.38×10^{-5}	0.75×10^{-14}	$(1.1\pm0.5)\times10^{14}$
$7s$	63.43	2.49×10^{-4}	6.36×10^{-4}	2.78×10^{-5}	0.78×10^{-13}	$(1.0\pm0.5)\times10^{-13}$
$7p$	114.35	7.65×10^{-5}	4.74×10^{-4}	2.08×10^{-8}	0.002×10^{-13}	3×10^{-13}
$6d$	202.54	2.44×10^{-5}	3.56×10^{-4}	1.38×10^{-14}	0	$(1.1\pm0.3)\times10^{-12}$
$8s$	302.68	1.09×10^{-5}	2.91×10^{-4}	3.25×10^{-22}	0	3.9×10^{-13}

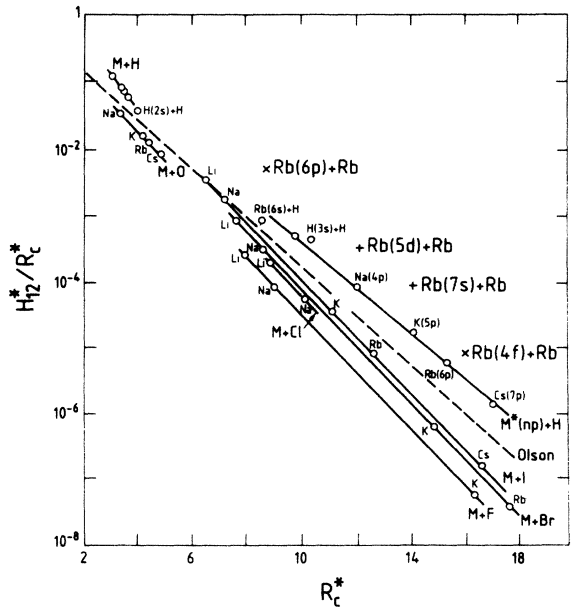

FIG. 5. Reduced variable plot of the ratio of the splitting to crossing radius as a function of crossing radius. Except for Rb data are reported from Ref. 18. For Rb (+) correspond to experimentally studied levels (×) only calculations.

$$R_c^* = \left[\frac{\alpha+\gamma}{2}\right] R_c$$

[where $\alpha=(2I_A)^{1/2}\gamma=(2I_B)^{1/2}$, I_A is the ionization potential of the covalent atom, I_B the electron attachment on the negative ion] and by plotting $H_{1/2}^*/R_c^*$ against R_c^*. Results deduced from experimental and theoretical work are reported on Fig. 5.[18] To account for this set of results Olson proposed the following law[19] based on theoretical work of Smirnov:[20]

$$H_{12}^* = 1.09 R_c^* e^{-0.86 R_c^*} . \tag{20}$$

H_{12} values deduced from Olson's law do not explain any of our experimental results.

In order to evaluate H_{12}, a more sophisticated approach has been proposed by Janev and Salin.[21] They calculated the coupling in a similar way to the one used by Smirnov [asymptotic forms are used to express the wave function $\chi_1(R)$ of the electron in the covalent state and the wave function $\chi_2(R)$ of the electron in the negative state perturbed by the positive ion] but also included the perturbation of the covalent electron by the other atom. The coupling is expressed analytically and is represented for an alkali-metal atom ($^1\Sigma$ ionic curve) by the relation

$$H_{12} = \frac{1}{2} N_1 R^{\frac{1}{\alpha}-1} e^{-\alpha R} (2l_1+1)^{1/2} \times N_2 \left[\frac{C_0}{2\beta}(\beta-\gamma)+\frac{1}{2}\left[1+\frac{\gamma}{\beta}\right]\right] , \tag{21}$$

where $\beta=\alpha+1/R$. This relation is valid only for $\alpha R \gg 1$. N_1 is the normalization constant for $\chi_1(R)$

$$N_1 = (2\alpha)^{1/\alpha}\left[\Gamma\left[\frac{1}{\alpha}+1_1+1\right]\Gamma\left[\frac{1}{\alpha}-1_1\right]\right]^{-1/2} . \tag{22}$$

N_2 is the normalization constant for $\chi_2(R)$ and is equal to 2.5 a.u. for Rb^-.[22] C_0 is a coefficient related to the diffusion of an electron by a Rb atom at low energy and is given by

$$C_0 = 2\beta\left[\frac{1}{L}+\frac{\pi\alpha_p\beta}{3L^2}+\frac{4\alpha_p}{3L}\beta^2 Ln\frac{\beta\alpha_p^{1/2}}{4}\right]^{-1} , \tag{23}$$

where α_p is the polarizability of the Rb atom [320 a.u. (Refs. 23 and 24) and L the diffusion length of the electron [27 a.u. (Refs. 25)].

H_{12} is calculated for each level using formula (21) and $k^-(nl)$ are deduced from these values. The theoretical values (Table IV) agree with measurements for the $5d$ and $7s$ levels. H_{12} values deduced from Olson's law give, respectively, $k^-(5d)=1\times10^{-16}$ cm^3s^{-1} and $k^-(7s)=3\times10^{-16}$ cm^3s^{-1}. The highest values of H_{12}^* are plotted on Fig. 5. They are at least ten times higher than those predicted by Olson's empirical law. Some remarks have to be made concerning the comparison between Olson and Janev approaches. In fact, formula (21) and Olson's law are similar for $\alpha\approx\gamma\approx0.5$ (i.e., $I_A\approx I_B\approx3.4$ eV). These values correspond approximately to the ionization potential of alkali-metal atoms and to the electron affinity of halogen atoms. Figure 6 shows that the coupling H_{12} is lower than Olson's prediction for the highest ionization potentials and electron affinities (alkali + halogen) and higher for the lowest potentials and electron affinities (resonant alkali-metal atoms, $I_A=2.5$–3 eV and hydrogen, $I_B=0.75$ eV). It is therefore not surprising that for the ionization potential of the Rb(nl) atoms ($I_A\approx0.5$ eV) and the electron affinity of Rb $I_B=0.49$ eV) H_{12} is ten times higher.[26]

Calculated rate coefficients are much lower than measured values for the $7p$, $6d$, and $8s$ levels: the crossing point is passed diabatically (i.e., $P_{12}\approx0$). No crossing occurs for the $7d$ and $9s$ levels. The use of the LSZ theory in its simpliest form is no longer valid: another mechanism must be proposed.

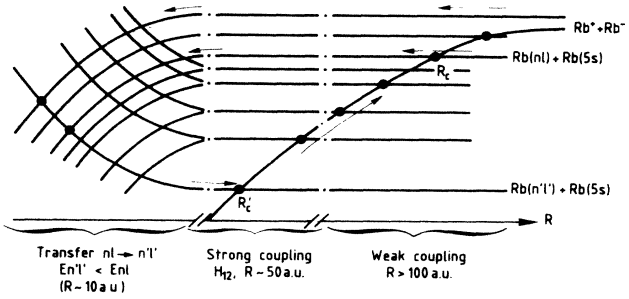

FIG. 6. Schematic representation of the ion-pair formation mechanism for levels above $7s$.

In Fig. 6 we propose a possible mechanism in order to explain the results obtained for the highest levels. In the initial covalent state no coupling with the ionic curve exists (i.e., no crossing or the value for H_{12} is negligible). At short internuclear distances the various covalent curves are coupled leading to a possible transfer to a $n'l'$ configuration of lower energy. The output channel $n'l'$ crosses the ionic curve with a higher probability $P_{12}(n'l')$. The total probability for ion pair formation from the $n'l'$ level is the following:

$$P_{n'l'}=[1-P_{12}(n'l')]\prod_{n''l''(>n'l')}^{5g}P_{12}(n''l'')$$

($5g$ is the highest level for which a crossing with the ionic curve is possible), where $P_{12}(n'l')$ is calculated for the threshold velocity with formula (19). $P_{n'l'}$ values for the various levels are given in Fig. 7. Such a mechanism relates the cross section for ion-pair formation $\sigma^-(nl)$ to the cross sections for collisional transfer $\sigma_{nl\to n'l'}$

$$\sigma^-(nl)=\sum_{n'l'(<nl)}P_{n'l'}\sigma_{nl\to n'l'}\ .$$

The $P_{n'l'}$ values show that the $5d$ and $6p$ levels are the most important for ion-pair formation. In order to estimate the corresponding transfer cross sections an average value for $\sigma_{nl\to 5d,6p}$ is defined, such that

$$\sigma^-(nl)=\sigma_{nl\to 5d,6p}(P_{5d}+P_{6p})$$

and as $P_{5d}+P_{6p}=0,97$ we have $\sigma_{nl\to 5d,6p}\simeq\sigma^-(nl)$.

The collisional transition results in considerable energy conversion from the internal energy of the excited level nl into kinetic energy (more than 2000 cm^{-1}). For the lowest level Rb($7p$), $\sigma_{7p\to 5d,6p}$ is 2 orders of magnitude lower than the quenching cross section estimated to be given by the geometrical cross section.[27]

This result seems to be reasonable, since the quenching mainly corresponds to the transfer towards neighboring levels (in this case, $4f$ and $6d$). For highest level $\sigma_{nl\to 5s,6p}$ decrease exponentially with the energy defect of the reaction.

Finally it is interesting to refer to alkali-halogen mixtures experimental results. Near threshold they are analyzed in terms of the LSZ theory and compared to a universal LSZ curve.[28] This curve represents the variation of a reduced cross section $Q/4\pi R_c^2$ with a reduced velocity $v/\delta_0(\delta_0=2\pi H_{12}^2R_c^2)$, Fig. 8. Q values do not take into account the fact that the different covalent molecular states are not all coupled with the ionic states and must be consequently reduced to be compared to the experimental results. In the Rb(nl)Rb($5s$) system H_{12} values are calculated for the $5d$ and $7s$ system from Janev and Salin and consequently it is easy to deduce $Q(5d)$ and $Q(7s)$ from the universal LSZ curve. In this system the statistical reduction of the Q values comes from the fact that ion-pair formation occurs along a $^1\Sigma^+$ state and only covalent curves with this symmetry are coupled to the ionic curve as long as only the radial coupling is taken into account. The $7s$ level corresponds to $^{1,3}\Sigma^+$ molecular states and the $5d$ level to $^{1,3}\Sigma^+$, $^{1,3}\Pi$, and $^{1,3}\Delta$ states. Experimental cross sections $\sigma^-(7s)$ and $\sigma^-(5d)$ are then multiplied by 4 and 20, respectively, to be compared to $Q(7s)$ and $Q(5d)$. There is a fair agreement between experimental values and theoretical predictions. The $5d$ level correspond to a v/δ_0 values near the maximum of the universal curve $[(v/\delta_0)_{max}=2.36$ (Ref. 29)]. As R_c values in Rb are higher than in alkali-halogen mixtures, high cross section

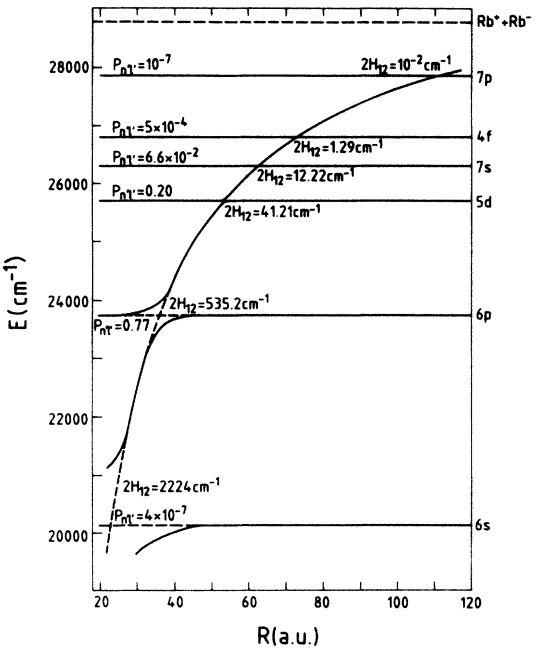

FIG. 7. Splitting $2H_{12}$ and probabilities $P_{n'l'}$ for ion-pair formation for levels below $7p$.

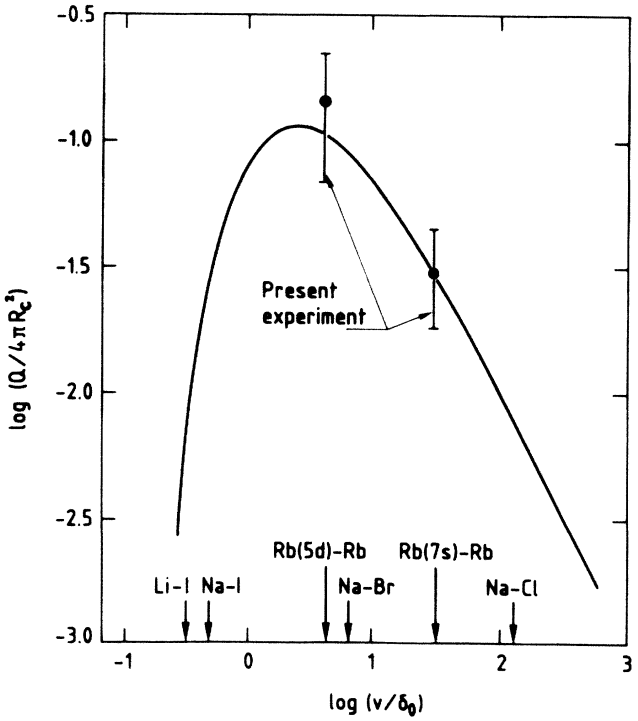

FIG. 8. Universal LSZ curve. The arrows denote the threshold for different colliding partners.

values are obtained. Variation of the Rb($5d$) and Rb($7s$) cross section with the energy seems to be interesting to study in order to check elaborate theories such as the close-coupling calculations performed by Faist and Levine[30] for alkali-halogen mixtures.

VIII. CONCLUSION

Ion-pair formation due to collisions between ground-state and excited-state alkali atoms has been clearly observed for the first time. This reaction does not significantly contribute to the formation of positive ions: $k^-(nl)$ has a maximum value of 10^{-14} cm^3 s^{-1} and k_{PI} is of the order of 10^{-8} cm^{-3} s^{-1}. The measured rate coefficients provide direct information about the reaction mechanism and the coupling at the crossing point between the ionic and the covalent curves.

This process is expressed in terms of a simple electron transfer from the orbital of the excited atom to the orbital of the negative ion for the $5d$ and $7s$ levels. This process fulfills the criteria for the application of the LZS formalism. As already explained, Olson's law cannot be applied to the Rb + Rb(nl) system; however, the coupling H_{12} is well accounted for the Janev and Salin formalism.

In the case of intermediate states ($7p$ to $9s$), crossings of molecular states at short internuclear distances may account for the ion-pair formation. We are presently checking the proposed mechanism by looking at the following channels:

$$K(nl)+\mathrm{Rb}\rightarrow K^+ + \mathrm{Rb}^-$$

$$K(nl)+\mathrm{Rb}\rightarrow K^- + \mathrm{Rb}^+$$

in a K-Rb gas-phase mixture.

Finally, for the highest Rb levels (i.e., above $8d$) negative ions observed can be simply explained by radiative cascade.

ACKNOWLEDGMENT

The authors are indebted to Dr. F. Gounand for critical discussion and valuable comments of the manuscript.

[1]Y. T. Lee and B. H. Mahan, J. Chem. Phys. **42**, 2893 (1965).
[2]G. V. Marr and S. R. Wherret, J. Phys. B **5**, 1735 (1972).
[3]M. Klewer, M. J. M. Beerlage, J. Los, and M. J. Van der Wiel, J. Phys. B **10**, 2809 (1977).
[4]M. Chéret, L. Barbier, W. Lindinger, and R. Deloche, J. Phys. B **15**, 3463 (1982). M. Chéret and L. Barbier, J. Phys. **46**, C1-193 (1985).
[5]M. Chéret and L. Barbier, Phys. Rev. A **30**, 1132 (1984).
[6]P. Frey, F. Breyer, and H. Hotop, J. Phys. B **11**, L589 (1978).
[7]B. M. Smirnov, *Negative Ions* (McGraw-Hill, New York, 1982).
[8]J. M. Goodings, J. M. Jones, and D. A. Parkes, Int. J. Mass. Spectrom. Ion Phys. **9**, 417 (1972).
[9]W. P. West, T. B. Cook, F. B. Dunning, R. D. Rundel, and R. F. Stebbings, J. Chem. Phys. **60**, 5126 (1974).
[10]L. Barbier and M. Cheret, J. Phys. B **16**, 3213 (1983). It has been checked that the crossing between the $5p+5p$ covalent curve and the ionic curve plays a negligible role in the energy pooling reaction: Rb($5p$)+Rb($5p$)→Rb($5d$)+Rb($5s$).
[11]F. Gounand, J. Phys. **40**, 457 (1979).
[12]J. Marek and P. Munster, J. Phys. B **13**, 1731 (1980).
[13]A. Lindgard and S. E. Nielsen, At. Data Nucl. Data Tables **19**, 533 (1977).
[14]L. Landau, Phys. Z. Sowjetunion **2**, 46 (1932); C. Zener, Proc. Roy. Soc. London Ser. A **137**, 696 (1932); E. C. G. Stueckelberg, Helv. Phys. Acta **5**, 369 (1932).
[15]A. M. C. Moutinho, J. A. Aten, and J. Los, Physica **53**, 471 (1971); R. H. Neynaber and S. Y. Tang, J. Chem. Phys. **72**, 6176 (1984); D. P. Wang, S. Y. Tang, and R. H. Neynaber, J. Phys. B **18**, L513 (1985).
[16]J. Van den Bos, J. Chem. Phys. **52**, 3254 (1970).
[17]S. A. Adelman and D. R. Herschbach, Mol. Phys. **33**, 793 (1977).
[18]R. Grice and D. R. Herschbach, Mol. Phys. **27**, 159 (1974).
[19]R. E. Olson, F. T. Smith, and E. Bauer, Appl. Opt. **10**, 1848 (1971).
[20]B. M. Smirnov, Sov. Phys. Dokl. **10**, 218 (1965).
[21]R. K. Janev and A. Salin, J. Phys. B **5**, 177 (1972).
[22]E. Clementi and C. Roetti, At. Data Nucl. Data Tables **14**, 177 (1974).
[23]P. Foentealba, J. Phys. B **15**, L555 (1982).
[24]R. W. Molof, H. L. Schwartz, T. H. Miller, and B. Bederson, Phys. Rev. A **10**, 1131 (1974).
[25]M. Hugon, F. Gounand, P. R. Fournier, and J. Berlande, J. Phys. B **16**, 2531 (1983).
[26]It would be useful to check the theoretical models for reactions involving negative ions with a very low-electron attachment such as He$^-$(^4P) (0.07 eV).
[27]M. Hugon, F. Gounand, and P. R. Fournier, J. Phys. B **13**, L109 (1980).
[28]J. Los and A. W. Kleyn, *Alkali halide vapors structure spectra and reaction dynamics,* (Academic, New York, 1979), Chap. 8.
[29]A. P. M. Baede, Adv. Chem. Phys. **30**, 463 (1975).
[30]M. B. Faist and R. D. Levine, J. Chem. Phys. **64**, 2953 (1976).